Laser Chem., Vol. 15, pp. 229–247
Reprints available directly from the Publisher
Photocopying permitted by license only

PROTON TUNNELING IN 5-CHLOROTROPOLONE-M_1 (M = Kr, Xe, CH_4) VAN DER WAALS COMPLEXES

HIROSHI SEKIYA, TAIJI NAKAJIMA, HIDENORI HAMABE, AKIRA MORI, HITOSHI TAKESHITA and YUKIO NISHIMURA

Institute of Advanced Material Study, and Department of Molecular Science and Technology, Graduate School of Engineering Sciences, Kyushu University, Kasuga-shi, Fukuoka 816, Japan

(Received March 11, 1994)

The S_1-S_0 fluorescence excitation spectra of 5-chlorotropolone-M_1 (M = Kr, Xe, CH_4) van der Waals (vdW) complexes in the region near the electronic origin have been measured in a supersonic free jet to investigate the effect of the vdW interactions on proton tunneling. Tunneling splittings have been observed in the vdW vibrations as well as in the 0_0^0 transitions of the Kr and Xe complexes. The 0_0^0 tunneling splitting of the 5-chlorotropolone-$(CH_4)_1$ complex is significantly smaller than those of the Kr and Xe complexes. It has been suggested that the vdW vibrations couple with intramolecular motions, leading to a higher potential energy barrier to tunneling in the CH_4 complex. The results of the 5-chlorotropolone complexes have been compared to those of the tropolone complexes.

KEY WORDS: Fluorescence excitation spectrum, 5-chlorotropolone, vdW complexes, proton tunneling.

1. INTRODUCTION

Proton tunneling in the tropolone (TRN) molecule has been studied extensively in rare gas matrices,[1,2] in the gas phase,[3–5] and in supersonic free expansions.[6–10] Tunneling splittings measured in the condensed phases are very different from those in the isolated states. For example, Alves and Hollas[1–3] observed tunneling splittings in the $\tilde{A}^1B_2$–$\tilde{X}^1A_1$ absorption spectrum of TRN in the gas phase.[1–3] The tunneling doublet separations $|\Delta'_0 - \Delta''_0|$ of the 0_0^0 transition were measured to be 18.9 and 2.2 cm^{-1}, respectively, for tropolone-OH (TRN(OH)) and tropolone-OD (TRN(OD)), where Δ'_0 and Δ''_0 are the tunneling splittings in the zero-point levels of the $\tilde{A}$ and $\tilde{X}$ states, respectively. The corresponding values in the fluorescence excitation spectra of TRN(OH) and TRN(OD) in neon matrix are 21 and 7 cm^{-1}, respectively.[2] Redington and Redington[1] measured the infrared matrix-isolation spectra in a neon matrix. They estimated the Δ''_0 values of TRN(OH) and TRN(OD) in the $\tilde{X}$ states to be 2.2 and 3 cm^{-1}, respectively. Recently, the Δ''_0 value of TRN(OH) has been measured to be

0.99 cm^{-1} by Tanaka et al.[11] The Δ''_0 value for TRN(OD) in the isolated state is expected to be very small ($<< 1\ cm^{-1}$) compared to Δ''_0 of TRN(OH), because temperature dependence of the relative intensity of the two tunneling doublet components in the fluorescence excitation spectrum of jet-cooled molecule is very small.[6,9]

The differences in the tunneling splittings of the condensed phase and the isolated state suggest that the solvent molecules give perturbation to proton tunneling. These experimental data stimulated us to investigate proton tunneling in clusters. The magnitude of tunneling splitting is very sensitive to the changes in the geometry of TRN.[7–10] The changes in the tunneling splittings of vibronic states of vdW clusters compared to those of the bare molecule may provide additional information about the intermolecular interactions, which have not been obtained from various vdW complexes of the aromatic molecules.[12]

Intermolecular vdW vibrations have been measured in pdFB-Ar,[13,14] benzene-M (M = Ar, H_2O, CH_4, NH_3),[15] aniline-Ar,[16] chlorobenzene-Ar,[16] phenol-Ar,[16] fluorobenzene-Ar,[16] s-tetrazine-Ar,[17] aniline-Rg (Ar, Kr, Xe),[18] phenol-Rg,[18] chlorobenzene-Rg,[18] toluene-Rg,[18] s-tetrazine-Rg,[19] and carbazole-Kr.[20] Direct data obtained from the electronic spectra of these molecules are intermolecular frequencies and spectral shifts of the origin band relative to the bare molecule. In a TRN-M_1 complex, the solvent molecule M induces a change in the electron density of the π orbitals of TRN. In addition to proton motion, rearrangements of the skeletal atoms are necessary for proton transfer, therefore, the change in the π electron density may influence the proton transfer process. If the intermolecular interactions of M with TRN affect the intramolecular normal modes of TRN, the effective height of the potential energy barrier to tunneling may change, leading to decreased or increased tunneling splitting.

Previously, we reported preliminary results on the S_1-S_0 fluorescence excitation spectra of the TRN(OH)-Rg_1 (Rg = Ar, Kr, Xe) vdW complexes and their OD derivatives in the region near the electronic origin.[21] Intermolecular vibrations were observed in these spectra and the assignments of transitions were given. The H/D isotope effect on the vibrational frequencies and the temperature dependence of vibrational distribution provided unambiguous assignments of the tunneling splittings. The decrease of the tunneling splitting was observed in a bending mode of TRN(OD)-Kr_1 and TRN(OD)-Xe_1.

The aim of this work is to investigate the effect of the intermolecular interactions on proton tunneling of 5-chlorotropolone (5CTR). We have measured the fluorescence excitation spectra of the 5CTR-M_1 (Kr, Xe, CH_4) vdW complexes. The S_1-S_0 electronic spectra of jet-cooled 5CTR were investigated by us.[22] The 0_0^0 tuneling splitting of 5CTR(OH) was determined to be 23 cm^{-1}, which is slightly larger than that of TRN(OH).[23] The tunneling splittings of vdW vibrations have been observed in the 5CTR(OH)-Kr_1 and 5CTR(OH)-Xe_1 spectra. The tunneling splittings of the 5CTR-M_1 (M = Kr, Xe, CH_4) complexes have been compared to those of the TRN-M_1 (M = Ar, Kr, Xe, CH_4) complexes. It has been found that the attachment of CH_4 to the seven-membered ring significantly decreases the 0_0^0 tunneling splitting.

2. EXPERIMENTAL

The experimental apparatus was essentially the same as that used for our study of the tropolone-Rg vdW complexes.[21] 5CTR(OH) was synthesized following a known procedure.[24] 5CTR(OH) was purified by recrystallization from ethanol and following sublimation. The 5CTR-M_1 (M = Kr, Xe, CH_4) complexes were prepared as follows. The Kr, Xe, and CH_4 gases were diluted with the helium gas in a vessel, and then further mixed with 5CTR(OH) in the pulsed nozzle housing. The concentration of M was controlled in the range 0.1–1%. 5CTR(OD) was prepared by introducing D_2O in the nozzle housing. The nozzle housing was heated with a coiled heater to increase the vapor pressure. The temperature in the nozzle housing was 120–150°C. The diameter of the nozzle was 300 μm. The S_1-S_0 transitions of the vdW complexes were excited with a XeCl excimer laser (Lambda Physik LPX100) pumped dye laser (Lambda Physik FL3002). The linewidth of the dye laser was 0.2–0.3 cm^{-1} (FWHM). The fluorescence signal was detected with a photomultiplier (Hamamatsu R955). The intensity of the dye laser was monitored with a photodiode to correct the fluorescence intensity for the variation of the dye laser power. These two signals were fed into a digital storage scope (Philips PM3323). The averaged signal was stored on a microcomputer (NEC PC9801), and recorded on a X-Y plotter as a function of the wavelength.

3. RESULTS

3.1 Fluorescence excitation spectrum of 5CTR-Kr_1.

Figure 1 shows the fluorescence excitation spectrum of 5CTR(OH)-Kr_1. The 0_0^0 transition of 5CTR-Kr_1 is observed at 25942.9 cm^{-1}, which is 66.8 cm^{-1} red-shifted relative to the electronic origin of the bare molecule. The red-shift of 5CTR(OH)-Kr_1 is similar to that of 72.2 cm^{-1} of TRN(OH)-Kr_1, indicating that the structure of 5CTR(OH)-Kr_1 is very similar to that of TRN(OH)-Kr_1 in which the Rg atom attaches to the seven-membered ring in the TRN-Rg_1 complexes.[21] The transitions marked with asterisks are assigned as hot bands of 5CTR(OH), because these transitions appear without introducing Kr. The lower frequency hot band and the higher frequency one are assigned to the 25_1^1 and 26_1^3 transitions, respectively, from the ν_{25} and ν_{26} frequencies in S_1 and S_0.[22,25] Several low frequency transitions in Figure 1 must be due to vdW vibrations, because these transitions have not been observed in the fluorescence excitation spectrum of 5CTR(OH).

We have examined temperature dependence of the relative intensity of low-frequency transitions, and the H/D isotope effect on frequencies to obtain an evidence for the existence of tunneling splittings in Figure 1. Figures 2a and 2b show the temperature dependence of the fluorescence excitation spectrum of 5CTR(OH)-Kr_1. Figure 2b was measured at relatively higher stagnation pressure and longer downstream distance, here the downstream distance is a length between the nozzle exit and the position laser beam crossing the molecular beam. By decreasing the

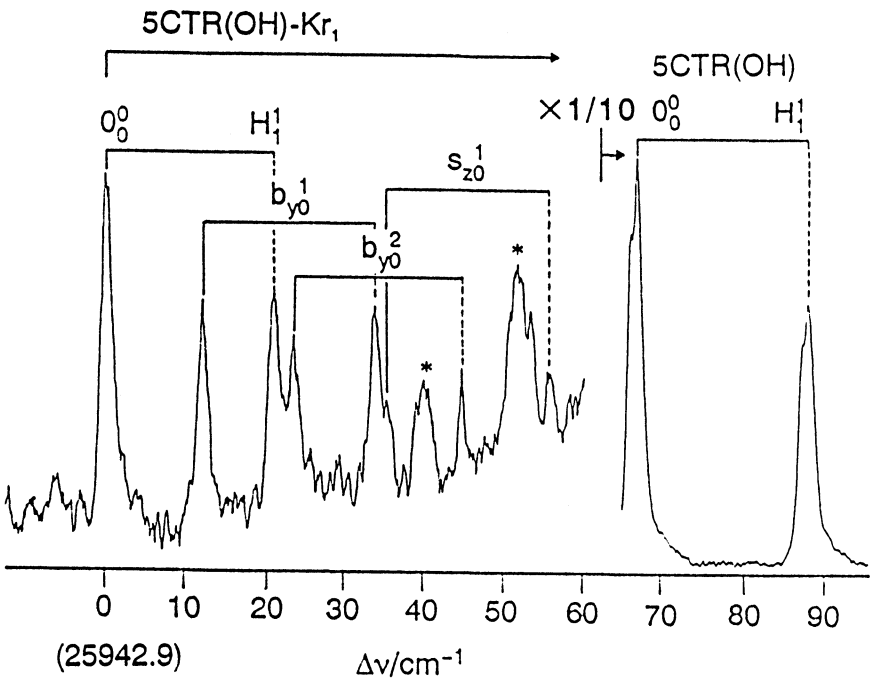

Figure 1 Fluorescence excitation spectrum of 5CTR(OH)-Kr_1 in the region near the electronic origin of the complex. The fluorescence intensity was corrected for variation of the wavelength dependence of the dye laser power. Broken lines indicate the H_1^1 transitions. The transitions denoted by asteriskes are hot bands of 5CTR(OH). The stagnation pressure and the downstream distance were 2.0 atm and 1.0 cm.

temperature, the intensities of the transitions at 21.1, 33.9 and 44.8 cm^{-1} decrease significantly compared to the other low-frequency transitions, suggesting that these transitions are originating from a thermally populated state in S_0. In contrast, the relative intensity increases in the transitions at 0, 12.2, 23.6 and 35.4 cm^{-1}. Thus, the former transitions are assigned as the H_1^1 (or $\bar{-}$) transitions, while the latter ones must be the H_0^0 (or $\bar{+}$) transitions, where H_1 and H_0 designate the higher wavenumber and lower wavenumber tunneling doublet components,[5,7] respectively. The separations between the following pairs of transitions observed at (0, 21.1 cm^{-1}), (12.2, 33.9 cm^{-1}), (23.6, 44.8 cm^{-1}), and (35.4, 56 cm^{-1}) are very similar to the 0_0^0 tunneling splitting (21.9 cm^{-1}) of 5CTR(OH), suggesting that the splittings of these transitions are due to proton tunneling. The H/D isotope effect on vibrational structure provides an evidence for the occurrence of proton tunneling, because the tunneling splitting of the OH complex should decrease significantly in the OD complex owing to the increase of the tunneling reduced mass.[2] The separations between the transitions of 5CTR(OH)-Kr_1 at 0 and 21.2 cm^{-1}, and 23.6 and 44.8 cm^{-1} decrease remarkably in the 5CTR(OD)-Kr_1 spectrum as is clear from Figure 3. The separations of the two doublets in the spectrum of 5CTR(OD)-Kr_1 are almost identical to the 0_0^0 tunneling splitting of 5CTR(OD). The b_{y0}^1 transition is observed at 12.2 cm^{-1} in Figure 1. The

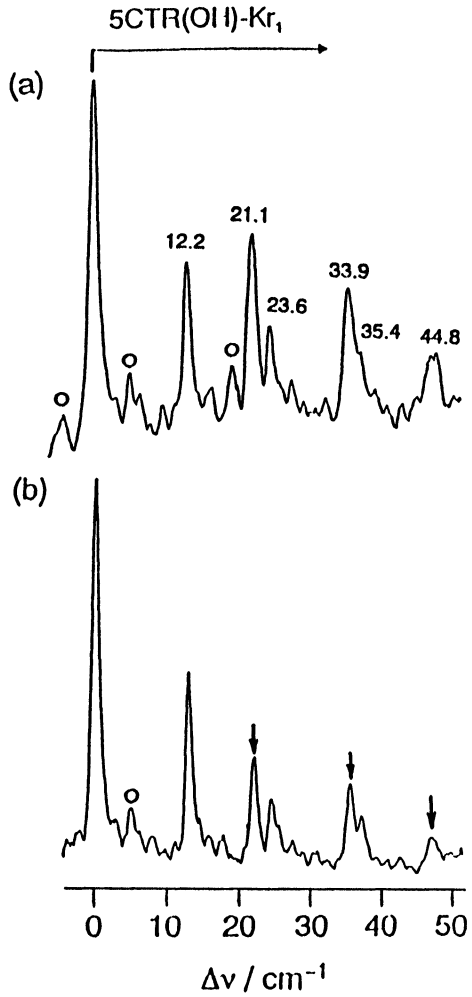

Figure 2 Temperature dependence of the vibrational distribution in the fluorescence excitation spectrum of 5CTR(OH)-Kr_1. The stagnation pressure and the downstream distance were 1.5 atm and 0.5 cm for (a), and 1.0 atm and 3.5 cm for (b), respectively. The transitions which show remarkable temperature dependence are indicated with arrows in (b). The transitions marked with open circles are due to 5CTR(OH)-Kr_2. The intensities of these transitions significantly depend on the concentration of Kr.

corresponding b_{y0}^1 transition of 5CTR(OD)-Kr_1 is not observed in Figure 3. The transition may overlap with the strong 0_0^0 transition of 5CTR(OH). Thus, we concluded that the splitting in the electronic origin band of 5CTR(OD)-Kr_1 must be due to proton tunneling.

We note that the vibrational structure in Figure 1 is similar to those in resonance enhanced multiphoton ionization (REMPI) spectra of substituted benzene-Rg_1 (Rg = Ar, Kr, Xe) complexes in the region near the electronic origin.[16,18] Mons et al.[18]

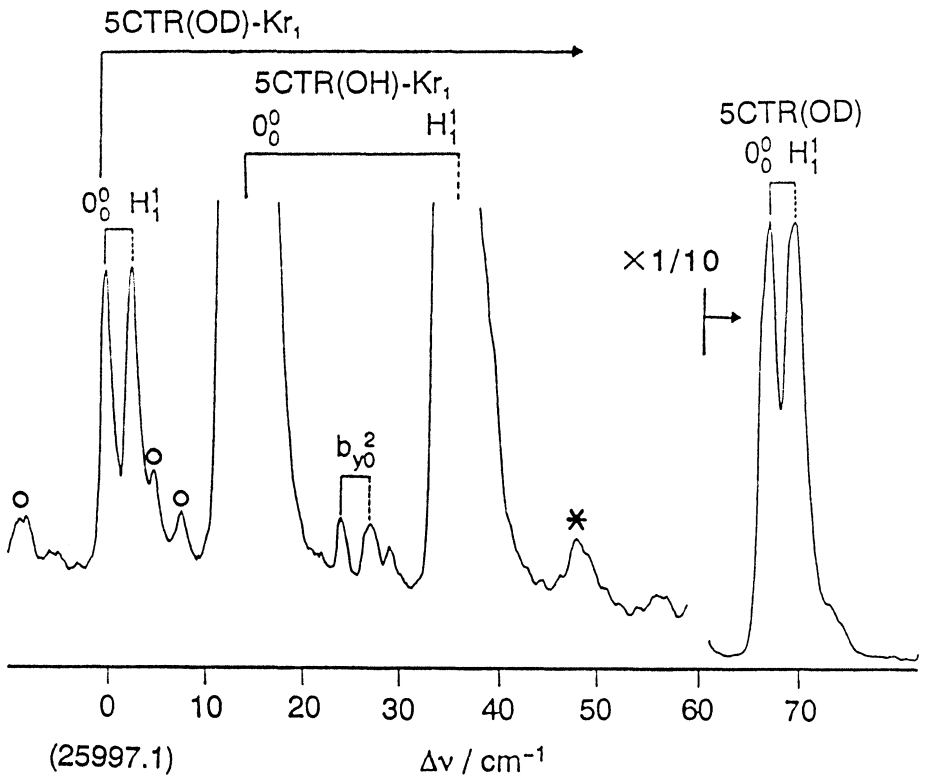

Figure 3 Fluorescence excitation spectrum of 5CTR(OD)-Kr_1. The fluorescence intensity was corrected for variation of the wavelength dependence of the dye laser power. Broken lines indicate the H_1^1 transitions. The transitions indicated by open circles are due to 5CTR(OD)-Kr_2. The transition denoted by asterisk is a hot band of 5CTR(OD). The stagnation pressure and the downstream distance were 1.5, atm and 0.5 cm.

measured REMPI spectra of chlorobenzene-Rg_1, phenol-Rg_1, and toluene-Rg_1. Prominent transitions in these spectra are associated with the one quantum transition of the symmetric bending (β'^1_0), the two quanta of the transition of the symmetric bending (β'^2_0), and the one quantum transition of the symmetric stretching (σ^1_0). In the C_s symmetry, the β in-plane bending mode (roughly parallel to the ring substitution) and the stretching (σ) belong to A′. The other asymmetric bending mode β'', in which Rg motion occurs along roughly short axis belongs to A″ class. Thus even harmonics are allowed transitions for the asymmetric bending mode. The highest symmetry of the 5CTR-Rg_1 complex is C_s on the assumption that symmetric proton transfer occurs.

In this work we use notations b_x, b_y, and s_z, for the asymmetric bending (x is roughly parallel to the short axis), the symmetric bending (y is roughly parallel to the long axis), and the stretching (perpendicular to the xy plane) modes, respectively.

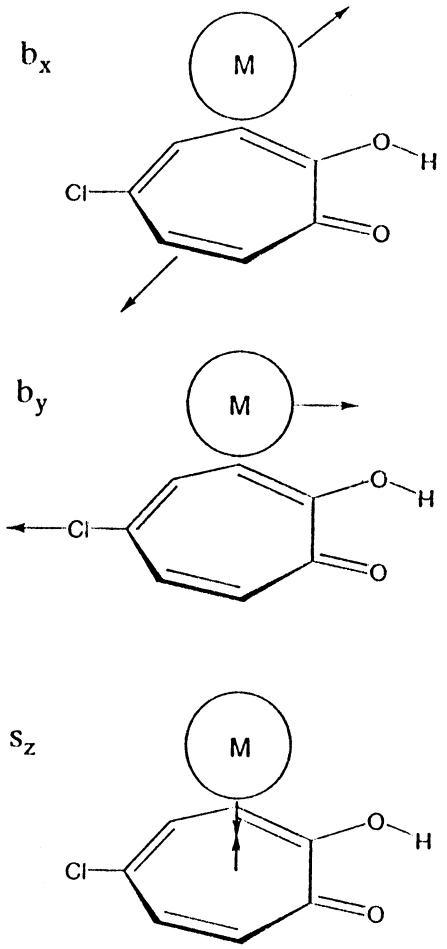

Figure 4 Schematic showing of the vdW vibration for the 5CTR-M complex.

These vdW vibrations in 5CTR(OH)-M are schematically shown in Figure 4. By analogy with the spectra of chlorobenzene-Rg_1[18] and TRN(OH)-Rg_1[21], the lowest frequency transition at 12.2 cm^{-1} in Figure 1 has been assigned to $b_{y0}^1 H_0^0$. Hereafter, we will abbreviate H_0^0 and designate b_{y0}^1. The frequency of the transition at 23.6 cm^{-1} is twice that of b_{y0}^1, and the transition at 23.6 cm^{-1} has been assigned to b_{y0}^2. Among the three H_0^0 transitions in Figure 1, the highest frequency transition at 35.4 cm^{-1} has been assigned to s_{z0}^1. The assignment of the corresponding H_1^1 transitions is straightforward. By analogy with the frequencies of the H_0^0 transitions in the spectrum of 5CTR(OH)-Kr_1, the assignment of the transitions in the spectrum of 5CTR(OD)-Kr_1 was performed. Frequencies of the observed transitions and their assignments are listed in Table 1.

Table 1 Fluorescence excitation spectra of 5CTR(OH)-Kr_1 and 5CTR(OD)-Kr_1.

Complex	*Wavenumber*	$\Delta\nu$ (cm^{-1})[a]	*Assignment*
5CTR(OH)-Kr_1	25942.9	0	0_0^0
	25955.1	12.2	b_{y0}^1
	25964.0	21.1	$0_0^0H_1^1$
	25966.5	23.6	b_{y0}^2
	25976.8	33.9	$b_{y0}^1H_1^1$
	25978.3	35.4	s_{z0}^1
	25982.8	39.9	25_1^1(5CTR(OH))
	25987.7	44.8	$b_{y0}^2H_1^1$
	25994.8	51.9	26_0^3(5CTR(OH))
	25998.9	56.0	$s_{z0}^1H_{sup}1$
	26009.7	66.8	0_0^0 (5CTR(OH))
	26031.6	88.7	$0_0^0H_1^1$(5CTR(OH))
5CTR(OD)-Kr_1	25997.1	0	0_0^0
	25999.7	2.7	$0_0^0H_1^1$
	26020.9	23.8	b_{y0}^2
	26023.6	26.5	$b_{y0}^2H_1^1$
	26064.6	67.5	0_0^0 (5CTR(OD))
	26067.2	70.1	$0_0^0H_1^1$ (5CTR(OD))

[a] Uncertainties are $\pm$ 0.3 cm^{-1}

3.2 Fluorescence excitation spectrum of 5CTR-Xe_1.

Figure 5 shows the fluorescence excitation spectrum of 5CTR(OH)-Xe_1. The 0_0^0 transition is observed at 25910.5 cm^{-1}. Several vdW vibrations are observed in Figure 5. The vibronic structure in the 5CTR(OH)-Xe_1 spectrum is similar to that in the 5CTR(OH)-Kr_1 spectrum.

Temperature dependence of vibrational distribution is shown in Figure 6. The relative intensity in the transitions at 20.5, 33.7, and 44.4 cm^{-1} decreases significantly with increasing the stagnation pressure and the downstream distance, suggesting that these transitions are the H_1^1 components. The transition at 33.7 cm^{-1} is very broad due to overlapping with two transitions. The transitions at 13.3 and 24.5 cm^{-1} are assigned as the H_0^0 components. By analogy with the spectrum of 5CTR(OH)-Kr_1, the assignment of the vdW vibrations in the spectrum of 5CTR(OH)-Xe_1 has been given, and the frequencies of the vdW vibrations and their assignments are listed in Table 2.

Figure 7 shows the fluorescence excitation spectrum of 5CTR(OD)-Xe_1. The electronic origin band is observed at 25962.6 cm^{-1}, which is 51.7 cm^{-1} blue shifted relative to the origin band of 5CTR(OH)-Xe_1. Three doublet splittings are observed in the spectrum of 5CTR(OD)-Xe_1. These splittings are due to tunneling, and have been assigned to 0_0^0, b_{y0}^1, b_{y0}^2 and their higher wavenumber tunneling doublet components. The results on TRN-Rg_1 and 5CTR-Xe_1 suggest that the frequencies of the vdW vibrations of the OD complexes are almost identical to those of the OH complexes. Thus, the transition at 35.0 and 37.8 cm^{-1} have been assigned to s_{z0}^1 and

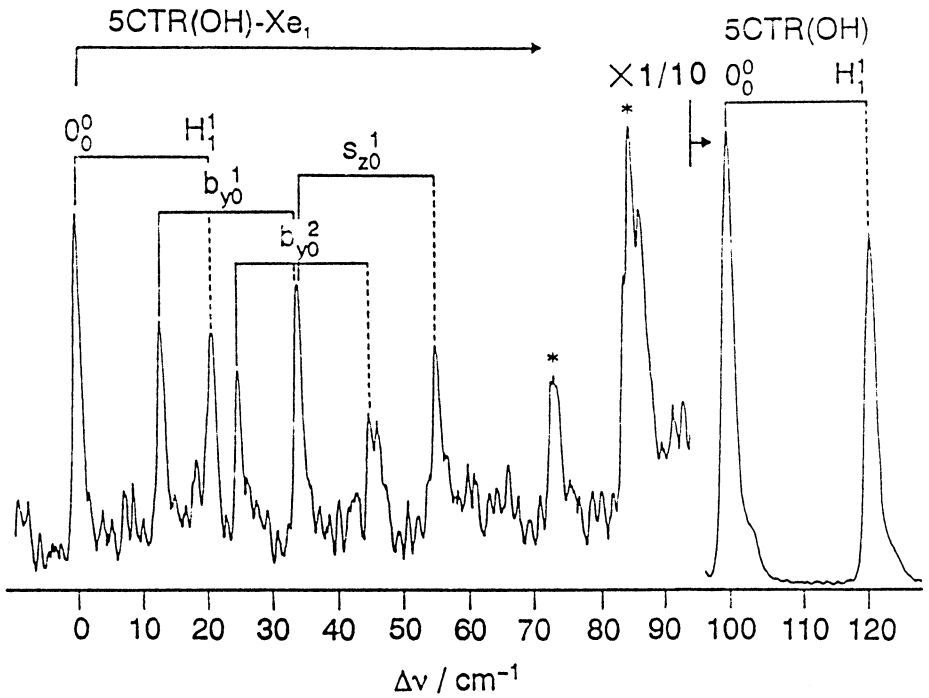

Figure 5 Fluorescence excitation spectrum of 5CTR(OH)-Xe_1 in the region near the electronic origin of the complex. The fluorescence intensity was corrected for variation of the wavelength dependence of the dye laser power. Broken lines indicate the H_1^1 transitions. The transitions denoted by asterisks are hot bands of 5CTR(OH). The stagnation pressure and the downstream distance were 1.5 atm and 0.5 cm.

$s_{z0}^1H_1^1$, respectively. The intensity of s_{z0}^1 is much larger than that of $s_{z0}^1H_1^1$. Relatively broad band width of s_{z0}^1 suggests that an unidentified transition is overlapped with s_{z0}^1.

3.3. Fluorescence excitation spectrum of 5CTR-$(CH_4)_1$

Figure 8 shows the fluorescence excitation spectrum of 5CTR(OH)-$(CH_4)_1$. The 0_0^0 transition is observed at 25939.4 cm^{-1}. Vibronic transitions are observed at 17.0, 29.1, 31.0. and 43.4 cm^{-1}. The temperature dependence of these transitions were measured to examine the existence of the H_1^1 transitions. Figure 9b was obtained by decreasing the temperature compared to Figure 9a. The intensity of the lowest frequency transition at 17.0 cm^{-1} in Figure 9a reduced remarkably in Figure 8b. The fluorescence excitation spectrum of 5CTR(OD)-$(CH_4)_1$ shown in Figure 10 was measured to assign the transition at 17.0 cm^{-1}. A prominent doublet splitting is observed at 25990.5 and 25992.5 cm^{-1}. The corresponding doublet splitting with a small separation (2 cm^{-1}) is not observed in the spectrum of 5CTR(OH)-$(CH_4)_1$. The temperature dependence of the vibrational distribution as well as the H/D isotope effect on the vibrational structure reveals that the transition at 17.0 cm^{-1} is $0_0^0H_1^1$ of 5CTR(OH)-$(CH_4)_1$.

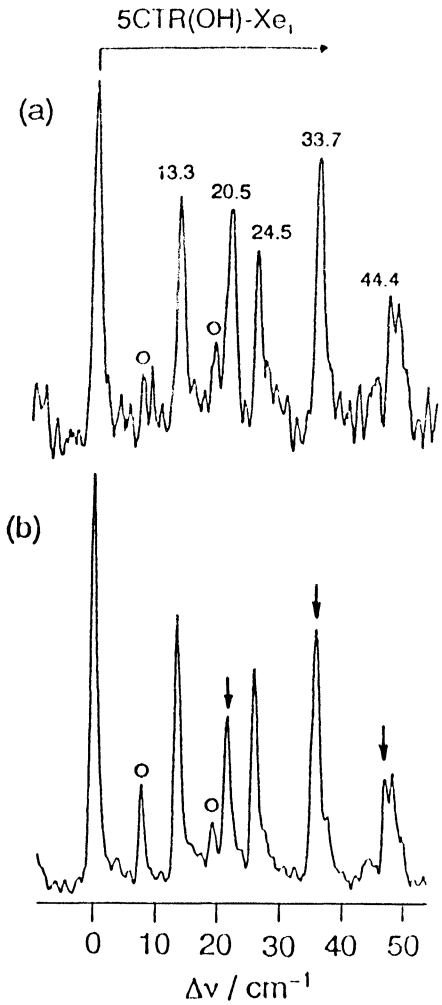

Figure 6 Temperature dependence of the vibrational distribution in the fluorescence excitation spectrum of 5CTR(OH)-Xe_1. The stagnation pressure and the downstream distance were 1.5 atm and 0.5 cm for (a), and 2.0 atm and 3.0 cm for (b), respectively. The transitions that show remarkable temperature dependence are indicated by arrows. Open circles indicate transitions due to 5CTR(OH)-Xe_2.

The transitions at 29.1 and 31.0 cm^{-1} in Figure 8 are probably due to vdW vibrations. The corresponding transitions of 5CTR(OD)-$(CH_4)_1$ are observed around 30 cm^{-1}, in which at least two transitions are overlapped each other. By analogy with the REMPI spectrum of benzene-$(CH_4)_1$ measured by Menapace and Bernstein,[15] the candidates for the transitions at 29.1 and 30.0 cm^{-1} in Figure 8 are bending and torsion modes.

Table 2 Fluorescence excitation spectra of 5CTR(OH)-Xe_1 and 5CTR(OD)-Xe_1.

Complex	*Wavenumber*	$\Delta\ \nu\ (cm^{-1})^a$	*Assignment*
5CTR(OH)-Xe_1	25910.9	0	0_0^0
	25923.2	13.3	b_{y0}^1
	25931.0	20.5	$0_0^0H_1^1$
	25935.0	24.5	b_{y0}^2
	25944.2	33.7	$b_{y0}^1H_1^1 + S_{z0}^1$
	25954.9	44.4	$b_{y0}^2H_1^1$
	25965.2	54.7	$s_{z0}^1H_1^1$
	25983.2	72.7	25_1^1 (5CTR(OH))
	25995.0	84.5	26_1^3 (5CTR(OH))
	26009.7	99.2	0_0^0 (5CTR(OH))
	26031.6	121.1	$0_0^0H_1^1$ (5CTR(OH))
5CTR(OD)-Xe_1	25962.6	0	0_0^0
	25964.9	2.3	$0_0^0H_1^1$
	25975.0	12.4	b_{y0}^1
	25977.3	14.7	$b_{y0}^1H_1^1$
	25981.8	19.2	25_1^1 (5CTR(OH))
	25989.1	26.5	b_{y0}^2
	25991.5	28.9	$b_{y0}^2H_1^1$
	25992.2	29.6	26_1^1 (5CTR(OH))
	25997.6	35.0	s_{z0}^1
	26000.5	37.8	$s_{z0}^1H_1^1$
	26009.7	47.1	$0_0^0H_1^1$ (5CTR(OH))
	26031.6	69.0	$0_0^0H_1^1$ (5CTR(OH))
	26064.6	102.0	0_0^0 (5CTR(OH))
	26067.2	104.6	$0_0^0H_1^1$ (5CTR(OH))

[a] Uncertainties are ± 0.3 cm^{-1}.

Table 3 Fluorescence excitation spectra of 5CTR(OH)-$(CH_4)_1$ and 5CTR(OD)-$(CH_4)_1$.

Complex	*Wavenumber*	$\Delta\ \nu\ (cm^{-1})^a$	*Assignment*
5CTR(OH)-$(CH_4)_1$	25939.4	0	0_0^0
	25956.4	17.0	$0_0^0H_1^1$
	25968.4	29.1	vdW mode
	25970.4	31.0	vdW mode
	25982.8	43.4	vdW mode
	26009.7	70.3	0_0^0(5CTR(OH))
	26031.6	92.2	$0_0^0H_1^1$
5CTR(OD)-$(CH_4)_1$	25990.5	0	0_0^0
	25992.5	2.0	$0_0^0H_1^1$
	26009.7	19.2	0_0^0 (5CTR(OH))
	26020.5	30.0	vdW mode
	26031.6	41.1	$0_0^0H_1^1$ (5CTR(OH))
	26064.6	74.1	0_0^0 (5CTR(OH))
	26067.2	76.7	$0_0^0H_1^1$ (5CTR(OH))

[a] Uncertainties are ± 0.4 cm^{-1}

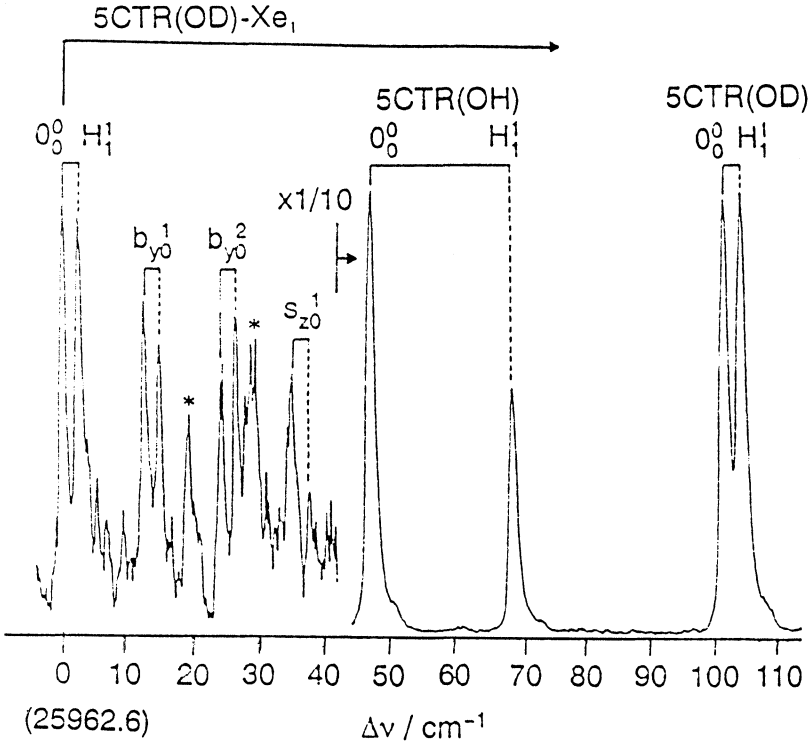

Figure 7 Fluorescence excitation spectrum of 5CTR(OD)-Xe_1 in the region near the electronic origin. The fluorescence intensity was corrected for variation of the wavelength dependence of the dye laser. Broken lines indicate the H_1^1 transitions. The stagnation pressure and the downstream distance were 2.0 atm and 3.0 cm.

4. DISCUSSION

4.1 Spectral shifts

Figure 11 shows the spectral shifts of 5CTR(OH)-M_1 versus the polarizability of M. For comparison, the spectral shifts of TRN(OH)-M_1 and TRN(OH)-M_2 are also shown in Figure 11. The 0_0^0 transitions of all the complexes are red-shifted with respect to 0_0^0 of the corresponding bare molecule, suggesting that the stabilization energy is larger in S_1 than in S_0 for all the complexes.

In Figure 11, a good linear correlation exists between the spectral red-shift and the polarizability of M. The binding energy of the complex involving a polar molecule is expressed by the sum of the dispersive and inductive interactions.[20] The strength of these interactions increases in proportion to the polarizability of M. The permanent dipole moment of TRN(OH) is μ (S_0) = 3.53 D,[26] while that of 5CTR(OH) has not been reported. The dipole moment of the ground-state 5CTR(OH) has been estimated to be 2.69 D for the C_{2v} structure by the semiempirical MO calculations,[27]

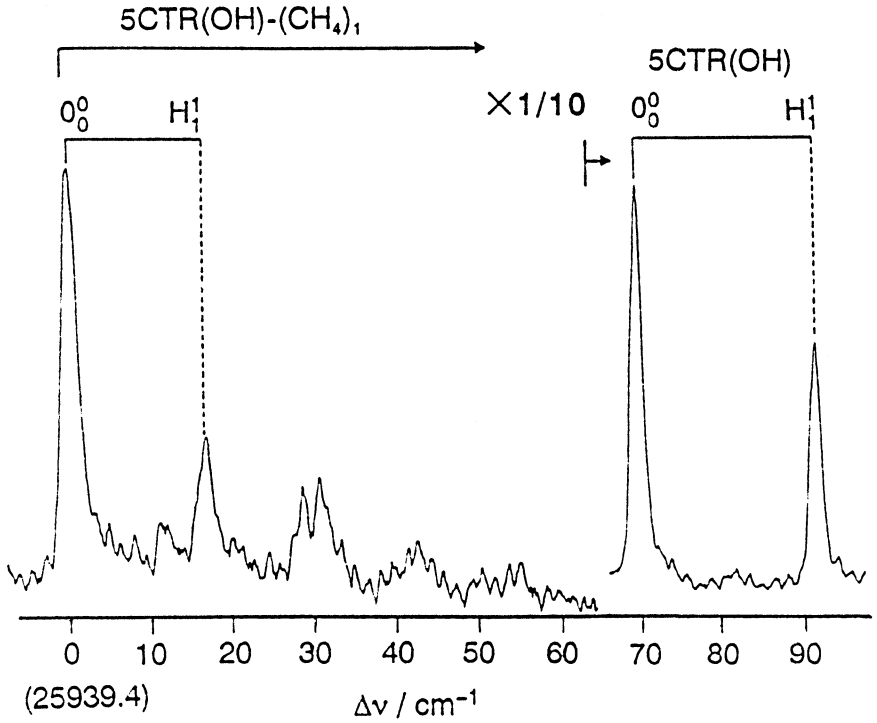

Figure 8 Fluorescence excitation spectrum of 5CTR(OH)-$(CH_4)_1$ in the region near the electronic origin of the complex. The fluorescence intensity was corrected for variation of the wavelength dependence of the dye laser power. Broken lines indicate the H_1^1 transitions. The stagnation pressure and the downstream distance were 1.5 atm and 0.5 cm.

where the MOPAC package (Ver. 6.01) furnished by Japanese Chemistry Exchange was used. We employed the PM3 approach for the determination of the minimum-energy molecular geometries of all the possible configurations.[28] 5CTR(OH) and TRN(OH) are polar molecules, therefore, the contribution of the inductive interactions as well as the dispersive interactions must be involved in the red-shifts in 5CTR(OH)-M_1 and TRN(OH)-M_1.

4.2 vdW Vibrations

The symmetric b_y and s_z modes are observed in the spectra of 5CTR-Kr_1 and 5CTR-Xe_1. The vibrational fundamentals of 5CTR-M_1 are summarized in Table 4 together with those of TRN-M_1. All the vibrational fundamentals of 5CTR(OH)-M_1 are smaller than the corresponding fundamentals of TRN(OH)-M_1. The decrease of the force constant as well as the increase in the reduces mass might be responsible for the reduction of the fundamental in each mode. We note that the vibrational structures of 5CTR-Rg_1 and TRN-Rg_1[21] are very similar to those of chlorobenzene-Rg_1[18] and phenol-Rg_1[18] except for the observation of the tunneling splittings in the former complexes. In these spectra, b_{y0}^1, b_{y0}^2, and s_{z0}^1 are dominant transitions. This suggests that

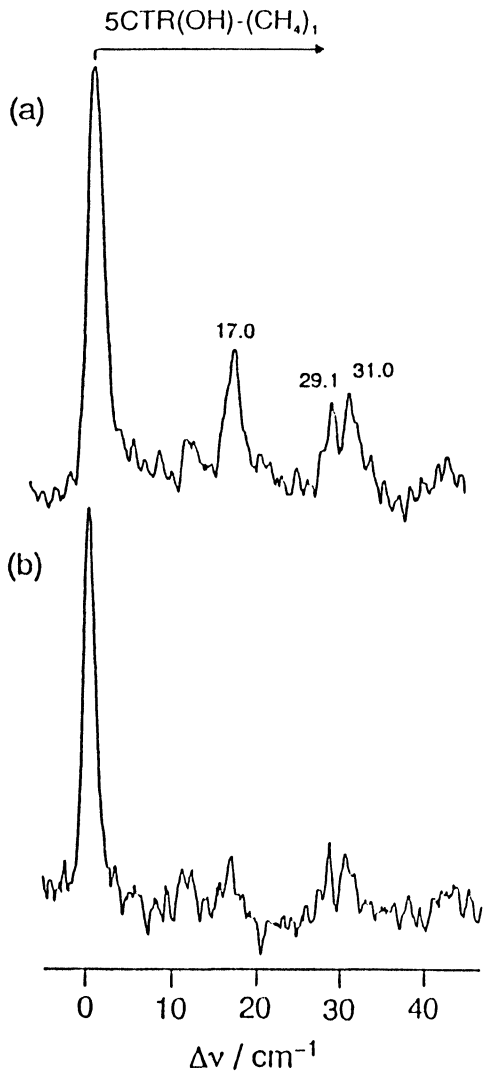

Figure 9 Temperature dependence of the vibrational distribution in the fluorescence excitation spectrum of 5CTR(OH)-$(CH_4)_1$. The stagnation pressure and the downstream distance were 1.5 atm and 0.5 cm for (a), and 2 atm and 3.5 cm for (b), respectively. The transition at 17.0 cm^{-1} is decreased remarkably in (b).

the symmetries of 5CTR-Rg_1 and TRN-Rg_1 are similar to those of the substituted benzene-Rg_1. The symmetries of 5CTR-Rg_1 and TRN-Rg_1 are probably near C_s.

The frequencies of b_{y0}^1 and b_{y0}^2 were measured to be 12.2, and 23.6 cm^{-1}, respectively, for 5CTR(OH)-Kr_1, and the corresponding values for 5CTR(OH)-Xe_1 are 13.3 and 24.5 cm^{-1}. On the basis of the observed values, the potential functions along the y axis for these complexes are almost harmonic in the lower energy region. In con-

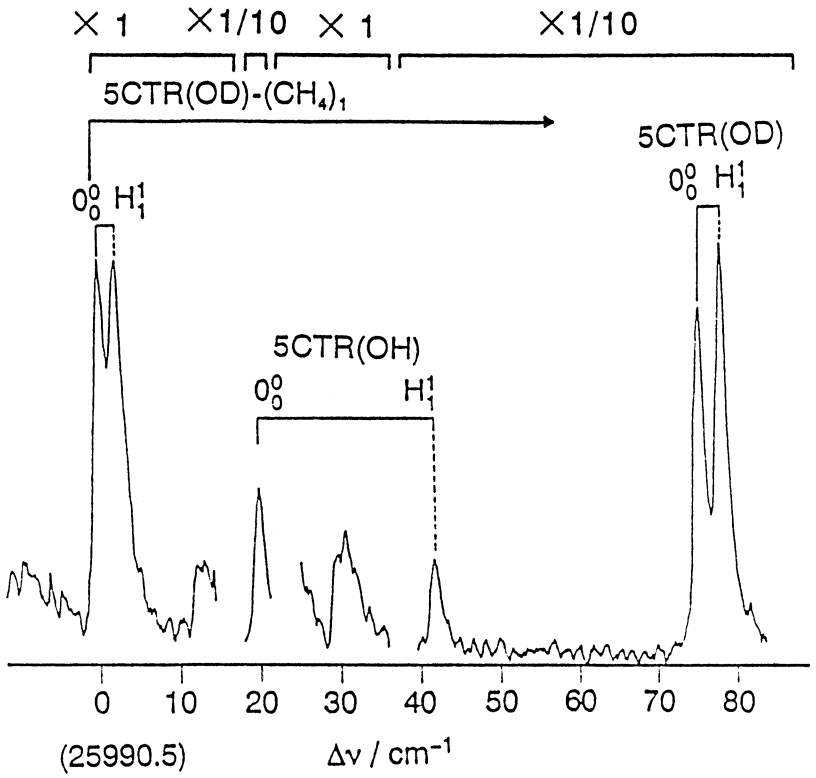

Figure 10 Fluorescence excitation spectrum of 5CTR(OH)-$(CH_4)_1$. The fluorescence intensity was corrected for variation of the wavelength dependence of the dye laser power. Broken lines indicate the H_1^1 transitions. The stagnation pressure and the downstream distance were 2.0 atm and 3.0 cm.

Table 4 Vibrational fundamentals (cm^{-1}) of the vdW modes in 5CTR-M and TRN-M.

Complex	ω (b_y)	ω (s_z)
5CTR(OH)-Kr	12.5	35.2
5CTR(OD)-Kr	11.9	
5CTR(OH)-Xe	13.3	34.4
5CTR(OD)-Xe	12.4	35.3
TRN(OH)-Ar[a]	17.4	
TRN(OH)-Kr[a]	17.7	39.5
TRN(OD)-Kr[a]	17.2	
TRN(OH)-Xe[a]	19.3	43.9
TRN(OD)-Xe[a]	20.0	41.2

[a] Reference 21.

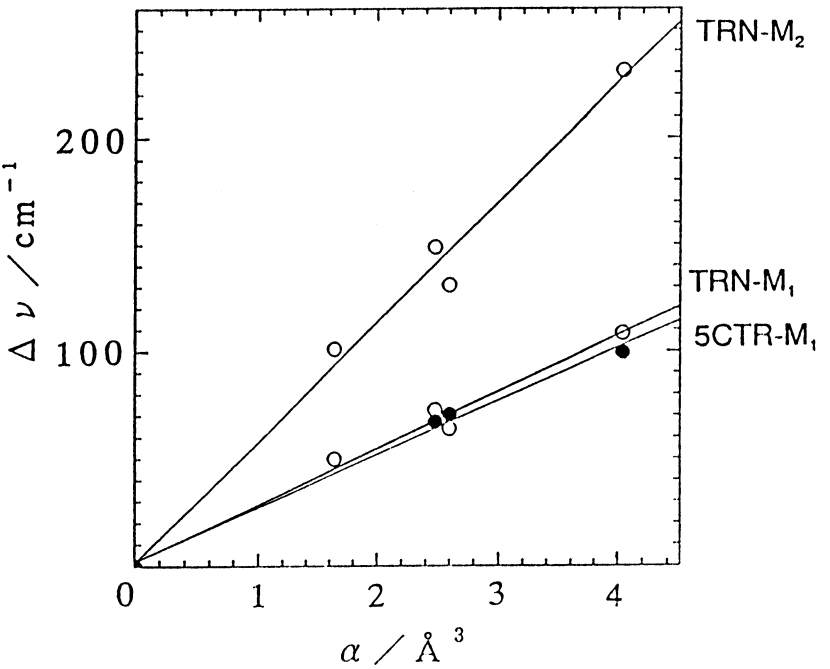

Figure 11 Spectral red-shifts of 5CTR(OH)-M_1, TRN(OH)-M_1, and TRN(OH)-M_2 relative to the corresponding bare molecule. The closed circles and open circles indicate the spectral shifts of 5CTR(OH)-M_1, and TRN(OH)-M_1 and TRN-M_2, respectively.

trast, the decrease of the b_y^2 frequency is significant for TRN(OH)-Rg_1. The frequencies of b_{y0}^1 and b_{y0}^2 are 17.9 and 23.6 cm^{-1}, and 19.1 and 34.0 cm^{-1} for TRN(OH)-Kr_1 and TRN(OH)-Xe_1, indicating that the b_y potential functions for these complexes are anharmonic. The harmonic b_y potential functions for 5CTR(OH)-Rg_1 must be a consequence of the interactions of substituted Cl atom with Rg, which balances asymmetric interactions due to the presence of the O-H-O chelate group in TRN(OH) and makes potential function relatively symmetric.

4.3 Tunneling splittings

Tunneling splittings in the spectra of 5CTR(OH)-M_1 are summarized in Table 5 together with those in the spectra of TRN(OH)-M_1. In Table 5, Δ'_v designates the tunneling splitting of the v state in S_1. The $|\Delta'_v - \Delta''_0|$ values of the vdW vibrations in 5CTR(OH)-Kr_1 are almost identical to $|\Delta'_0 - \Delta''_0|$ for the bare molecule, while the $|\Delta'_0 - \Delta''_0|$ values of 5CTR(OH)-Xe_1 decreased slightly. By comparing the intensity ratio $0_0^0H_1^1/0_0^0$ in the fluorescence excitation spectrum of 5CTR(OH) with that in the spectrum of TRN(OH), Δ''_0 of 5CTR(OH) was estimated to be 1 cm^{-1}.[22] The Δ''_0 value of 5CTR(OH)-Xe_1 is nearly 1 cm^{-1}, because the intensity ratio $0_0^0H_1^1/0_0^0$ in the 5CTR(OH)-Xe_1 spectrum is almost identical to that of 5CTR(OH). This suggests that the effective potential energy barrier to tunneling increases slightly in the S_1

Table 5 Tunneling splittings $|\Delta'_v-\Delta''_0|$ of 5CTR-M and TRN-M.

	$\lvert\Delta'_v-\Delta''_0\rvert$[a]			
Complex	0_0^0	b_{y0}^1	b_{y0}^2	s_{z0}^1
5CTR(OH)	21.9			
5CTR(OH)-Kr	21.1	21.7	21.2	20.6
5CTR(OH)-Xe	20.5	20.4	19.9	21.0
5CTR(OH)-CH_4	17.0			
5CTR(OD)	2.6			
5CTR(OD)-Kr	2.7		2.7	
5CTR(OD)-Xe	2.3	2.3	2.4	2.8
5CTR(OH)-CH_4	2.0			
TRN(OH)[b]	19.4			
TRN(OH)-Kr[b]	18.6	18.5	18.4	18.4
TRN(OH)-Xe[b]	17.8	18.1	19.2	17.7
TRN(OH)-CH_4	16.0			
TRN(OD)[b]	2.1			
TRN(OD)-Kr[b]	2.2	2.0	1.8	
TRN(OD)-Xe[b]	2.2	2.0	1.3	1.5
TRN(OD)-CH_4	1.6			

[a] Uncertainties are ± 0.34 cm^{-1}
[b] Reference 21.

state of 5CTR(OH)-Xe_1. Similar decrease of $|\Delta'_0 - \Delta''_0|$ is observed in TRN(OH)-Xe_1. The differences in the $|\Delta'_v - \Delta''_0|$ and $|\Delta'_0 - \Delta''_0|$ values are very small in 5CTR-Rg_1, although the $|\Delta'_v - \Delta''_0|$ values of b_{y0}^2 in TRN(OD)-Kr_1 and TRN(OD)-Xe_1 decrease significantly compared to those of the zero-point levels in TRN(OD)-Kr_1 and TRN(OD)-Xe_1. This difference might be related to the shape of the potential function along the y axis. As discussed previously, the potential functions for 5CTR-Rg_1 (Rg = Kr, Xe) along the y axis are more symmetric than those for TRN-Rg_1 (Rg = Kr, Xe).[21] Since the y axis is not exactly parallel to the C_2 axis of TRN, the change of the equilibrium position may induce asymmetry in the double-minimum potential well along the proton transfer coordinate in the case of the excitation of b_{y0}^2 in TRN(OD)-Kr_1 and TRN(OD)-Xe_1.

It should be noted that $|\Delta'_0 - \Delta''_0|$ of 5CTR(OH)-$(CH_4)_1$ is remarkably smaller than that of 5CTR(OH). The intensity ratio $0_0^0H_1^1/0_0^0$ for 5CTR(OH)-$(CH_4)_1$ is smaller than that of 5CTR(OH) under the same expansion conditions, showing that Δ''_0 increases slightly. The fluorescence excitation spectrum of TRN(OH)-$(CH_4)_1$ was similar to the spectrum 5CTR(OH)-$(CH_4)_1$. In this spectrum, $|\Delta'_0 - \Delta''_0|$ of TRN(OH)-$(CH_4)_1$ decreased by 4 cm^{-1} compared to that of TRN(OH), while no appreciable change in the intensity ratio $0_0^0H_1^1/0_0^0$ was observed in the spectra of TRN(OH)-$(CH_4)_1$ and TRN(OH). This suggests that the decrease in $|\Delta'_0 - \Delta''_0|$ is responsible for the reduction of Δ'_0 in TRN(OH)-$(CH_4)_1$. On the other hand, the reduction of $|\Delta'_0 - \Delta''_0|$ for 5CTR(OH) is ascribed to the decrease in Δ'_0 and/or increase in Δ''_0. The $|\Delta'_0 - \Delta''_0|$ value also decreases in 5CTR(OD)-$(CH_4)_1$ compared

to 5CTR(OD). The ratio $|\Delta'_0 - \Delta''_0|$ (complex)/$|\Delta'_0 - \Delta''_0|$ (bare molecule) for the OH species is similar to the OD species, implying that asymmetry in the double-minimum potential well is insignificant in the CH_4 complexes.

An explanation for the decrease in the $|\Delta'_0 - \Delta''_0|$ values of 5CTR-$(CH_4)_1$ and TRN-$(CH_4)_1$ is coupling of vdW vibrations with intramolecular motions of 5CTR(OH) and TRN(OH). It is known that low-frequency out-of-plane bending modes such as ν'_{25} and ν'_{26} of TRN(OH) remarkably decrease the tunneling splitting compared to the zero-point level in the S_1 state. The changes in the ν'_{25} and ν'_{26} modes due to a coupling with the vdW vibrations may increase or decrease in the height of the potential energy barrier. The slight decrease of $|\Delta'_0 - \Delta''_0|$ in 5CTR(OH)-Xe_1 also suggests the existence of a coupling of the vdW vibrations with intramolecular modes. The measurement of the vibrational frequency shifts and the tunneling splittings of the intramolecular modes in the TRN(OH) and 5CTR(OH) complexes may provide an evidence for the coupling. We are planning to measure the mass selected multiphoton ionization spectra of 5CTR-M_1 and TRN-M_1 to avoid heavy overlapping of the transitions of the complexes with those of the monomer.

5. CONCLUSION

The S_1-S_0 fluorescence excitation spectra of 5CTR-M_1 vdW complexes have been measured. The vdW vibrations are observed in these complexes. The vibronic structures of the 5CTR-Kr_1 and 5CTR-Xe_1 spectra are very similar to those of the chlorobenzene-Rg_1 complexes, suggesting that the symmetry of 5CTR-Rg is near C_s as a consequence of rapid proton transfer. The tunneling splittings of the vdW modes as well as the zero-point level have been measured. The tunneling splitting of the zero-point level of 5CTR–$(CH_4)_1$ decreases significantly compared to that of 5CTR, which is suggestive of the existence of the coupling between the vdW vibrations with intramolecular motion.

Acknowledgement

The authors wish to thank Miss Sayaka Ito for assistance of the synthesis of 5-chlorotropolone. We indebted to Mr. Hiroki Ujita for valuable discussions.

References

1. R. L. Redington and T. E. Redington, J. Mol. Spectrosc. **78**, 229 (1979)
2. R. Rossetti and L. E. Brus, J. Chem. Phys. **73**, 1546 (1980).
3. A. C. P. Alves and J. M. Hollas, Mol. Phys. **23**, 927 (1972).
4. A. C. P. Alves and J. M. Hollas, Mol. Phys. **25**, 1305 (1973).
5. A. C. P. Alves, J. M. Hollas, H. Musa and T. Ridley, J. Mol. Spectrosc. **109**, 99 (1985).
6. Y. Tomioka, M. Ito and N. Mikami, J. Phys. Chem. **87**, 4401 (1983).
7. R. L. Redington, Y. Chen, G. J. Scherer and R. W. Field, J. Chem. Phys. **88**, 627 (1988).
8. R. L. Redington, T. E. Redington, M. A. Hunter and R. W. Field, J. Chem. Phys. **92**, 6456 (1990).
9. H. Sekiya, Y. Nagashima and Y. Nishimura, J. Chem. Phys. **92**, 576 (1990).

10. H. Sekiya, Y. Nagashima, T. Tsuji, Y. Nishimura, A. Mori and H. Takeshita, J. Phys. Chem. **95**, 10311 (1991).
11. K. Tanaka, H. Honjo, T. Tanaka, H. Kouguchi, Y. Oshima and Y. Endo, in "Proceedings International Symposium on Molecular Spectroscopy", Ohio State University, 1992.
12. For a recent review see: M. R. Topp, Int. Rev. Phys. Chem. **12**, 149 (1993).
13. K. W. Butz, D. L. Catlett Jr., G. E. Ewing, D. Kranjnovich and C. S. Parmenter, J. Phys. Chem. **90**, 3553 (1986).
14. B. A. Jacobson, S. Humphrey and S. A. Rice, J. Chem. Phys. **89**, 5624 (1988).
15. J. A. Menpace and E. R. Bernstein, J. Phys. Chem. **91**, 2533 (1987).
16. E. J. Bieske, M. W. Rainbird, I. M. Atkinson and A. E. W. Knight, J. Chem. Phys. **91**, 752 (1989).
17. D. V. Brumbaugh, J. E. Kenny and D. H. Levy, J. Chem. Phys. **78**, 3415 (1983).
18. M. Mons, J. Le Calve, F. Piuzzi and I. Dimicoli, J. Chem. Phys. **92**, 2155 (1990).
19. P. M. Weber, J. T. Buontempo, F. Novak and S. A. Rice, J. Chem. Phys. **88**, 6082 (1988).
20. J. Boesiger and S. Leutwyler, Chem. Phys. Lett. **126**, 238 (1984).
21. H. Sekiya, T. Nakajima, H. Ujita, T. Tsuji, S. Ito and Y. Nishimura, Chem. Phys. Lett. **215**, 499 (1993).
22. T. Tsuji, H. Sekiya, Y. Nishimura, R. Mori, A. Mori and H. Takeshita, J. Chem. Phys. **97**, 6032 (1992).
23. The 0_0^0 tunneling splitting of 5CTR(OH) has been measured to be 21.9 cm^{-1}. The discrepancy between this value and a previous value of 23 cm^{-1} in reference 21 is due to larger bandwidth of the laser (0.8 ~1 cm^{-1}) than the present work.
24. T. Nozoe, S. Seto, S. Ebine and S. Ito, J. Am. Chem. Soc. **106**, 1895 (1951).
25. The transition at 26137 cm^{-1} in the fluorescence excitation spectrum of 5CTR(OH) reported in reference 21 has been assigned to the $25_0^1 26_0^1$ transition, which has provided the ν_{25} frequency in S_1.
26. M. Kubo, T. Nozoe and Y. Kurita, Nature **169**, 688 (1951).
27. H. Ujita, H. Sekiya and Y. Nishimura, unpublished results.
28. J. J. P. Stewart, J. Comp. Chem. **10**, 209 (1989).